

Targeting the menaquinol binding loop of mycobacterial cytochrome bd oxidase

Harikishore, Amaravadhi; Chong, Sherilyn Shi Min; Ragunathan, Priya; Bates, Roderick
Wayland; Grüber, Gerhard

2020

Harikishore, A., Chong, S. S. M., Ragunathan, P., Bates, R. W., Grüber, G. (2020). Targeting
the menaquinol binding loop of mycobacterial cytochrome bd oxidase. *Molecular Diversity*.
doi:10.1007/s11030-020-10034-0

<https://hdl.handle.net/10356/139176>

<https://doi.org/10.1007/s11030-020-10034-0>

This is a post-peer-review, pre-copyedit version of an article published in *Molecular
Diversity*. The final authenticated version is available online at:
<http://dx.doi.org/10.1007/s11030-020-10034-0>.

Downloaded on 09 Apr 2024 16:16:21 SGT

Targeting the Menaquinol binding loop of Mycobacterial Cytochrome *bd* Oxidase

Amaravadhi Harikishore¹, Sherilyn Shi Min Chong^{1,2,3}, Priya Ragunathan², Roderick W. Bates¹, and Gerhard Grüber^{2,*}

¹Division of Chemistry and Biological Chemistry, School of Physical and Mathematical Sciences, Nanyang Technological University, 21 Nanyang Link, Singapore 637371, Republic of Singapore

²School of Biological Sciences, Nanyang Technological University, 60 Nanyang Drive, Singapore 637551, Republic of Singapore

³Nanyang Institute of Technology in Health and Medicine, Interdisciplinary Graduate School, Nanyang Technological University, Republic of Singapore

*To whom correspondence should be addressed: Prof. Dr. Gerhard Grüber, Tel.: (65) 6316 2989; E-mail: ggrueber@ntu.edu.sg

Key Words: Tuberculosis, Mycobacteria, Cytochrome *bd* oxidase, OXPHOS pathway, Respiration, Drug Resistance

Abstract

Mycobacteria have shown enormous resilience to survive and persist by remodeling and altering metabolic requirements. Under stringent conditions or exposure to drugs, mycobacteria have adapted to rescue themselves by shutting down their major metabolic activity and elevate certain survival factor levels and efflux pathways to survive and evade the effects of drug treatments. A fundamental feature in this adaptation is the ability of mycobacteria to vary the enzyme composition of the electron transport chain (ETC), which generates the proton motive force for the synthesis of adenosine triphosphate via oxidative phosphorylation. Mycobacteria harbor dehydrogenases to fuel the ETC, and two terminal respiratory oxidases, an *aa3*-type cytochrome *c* oxidase (*cyt-bcc-aa3*) and a bacterial specific cytochrome *bd*-type menaquinol oxidase (*cyt-bd*). In this study, we employed homology modeling and structure based virtual screening studies to target mycobacteria specific residues anchoring the b558 menaquinol binding region of *Mycobacterium tuberculosis* *cyt-bd* oxidase to obtain a focused library. Furthermore, ATP synthesis inhibition assays were carried out. One of the ligands MQL-H₂ inhibited both NADH₂⁻, and succinate driven ATP synthesis inhibition of *M. smegmatis* inside-out vesicles in micromolar potency. Similarly, MQL-H₂ also inhibited NADH₂-driven ATP synthesis in inside-out vesicles of the cytochrome-*bcc* oxidase deficient *M. smegmatis* strain. Since neither varying the electron donor substrates nor deletion of the *cyt-bcc* oxidase, a major source of protons, hindered the inhibitory effects of the MQL-H₂, reflecting that MQL-H₂ targets the terminal oxidase cytochrome *bd* oxidase, which was consistent with molecular docking studies.

Introduction

The WHO 2019 report highlights that tuberculosis (TB) now accounts for more than a million deaths globally. The rise in incidence of multidrug resistant (MDR) or extremely drug resistant (XDR) organisms (74%) towards first line TB therapy coupled with increasing incidence of latent TB infections poses a serious threat to global health [1]. There has been a recent resurgence of drug discovery and development activities resulting in the addition of a number of new compounds to the TB-drug pipeline [2]. These include clofazimine and Q203 (Telacebec) targeting the NADH dehydrogenase (NDH; complex I) and cytochrome *c* oxidase (cyt-*bcc-aa3*) of the electron transport chain (ETC) [3, 4], and Sirturo (Bedaquiline; BDQ) [5] as well as the new generation of 3,5-dialkoxypyridine analogues of BDQ [6, 7], which inhibit ATP synthesis by the F-ATP synthase.

Within the ETC, the NDH and succinate dehydrogenases (SDHs; complex II) accept electrons from the donors NADH and succinate and transfer these electrons to the two terminal oxidases cytochrome-*bc₁:aa₃* oxidase supercomplex (cyt-*bc₁:aa₃*) and the cytochrome-*bd* oxidase (cyt-*bd*) via menaquinol [8]. The mycobacterial cyt-*bd* belongs to the long quinol/menaquinol binding domain (Q_L-loop) class [9]. The enzyme utilizes menaquinol as a substrate on the extracellular side for electron transfer and protons (derived from H₂O) on the intracellular side. Interestingly, cyt-*bd* was evolved to catalyse the reduction of molecular oxygen to water without the generation of reactive oxygen species (ROS) or protons [9, 10]. Its enzymatic turnover is sufficient to contribute the proton motive force (PMF) gradient resulting from the vectorial release of protons from the oxidation of menaquinol to the periplasm and the uptake of protons from the cytoplasm to form H₂O [11]. Mycobacterial cyt-*bd* encompasses three heme groups, a low spin Cytochromes *b*558, two high spin- *b*595 and a chlorin *d* as redox centers that conduct the partitioning of electron flux across the terminal oxidase. Homology to the closest structural bacterial homologs like *Geobacillus thermodenitrificans* [12] suggests that the subunits *b* and *d* are located within the bacterial cytoplasmic membrane. Two conserved glutamic acid residues, E99 and E107 in the related *Escherichia coli* enzyme, (Supplementary Fig. 1) were shown to anchor the heme *b*595 and play an important role in oxygen binding and reduction to water. Mutation of these two glutamate residues not only resulted in loss of oxidase activity but also loss of heme *b*595 and -*d*. Contrastingly, a similar mutation of conserved residue E257A (*E. coli*) located at the menaquinol binding site had inactivated the oxidase enzyme activity but without the loss of heme groups [11]. A very recent cryo-EM structure of the *E. coli* cyt-*bd* revealed an oxygen conducting channel (O-channel) comprising of hydrophilic residues such as S108(A), E107(A), and S140(A) and a proton channel outlined by conserved helix segment "WDGNQ" (TMH2(B))

to W63(B), which further extends and combines into O-channel [9]. These features highlight the presence of differential regulation node points, oxygen binding channel/proton channel inside this enzyme. Thus, cytochrome oxidases, positioned at a level upstream of the F-ATP synthase, are key to the maintenance of the proton motive force by catalyzing the flow of electrons for terminal reduction of molecular oxygen into H₂O and thereby ATP homeostasis. Genetic ablation of the cytochrome *bcc* complex in itself was not sufficient to induce cidal effects as the mycobacterial metabolic resilience enabled it to survive by elevating the levels of alternative non proton pumping terminal *cyt-bd* oxidase. Enhanced levels of *cyt-bd* expression has not only been shown to alleviate the membrane potential, but also to confer protection against hypoxia [13], CN [14], H₂O₂ [15], nitric oxide [16] and rescue from the cidal actions of antimycobacterials such as BDQ [17] or Q203 [18-20]. Studies employing genetic knock down or chemical inhibitors such as aurachin D [21] have shown the inhibition of the *cyt-bd* mediated increase in oxygen consumption rate (OCR) further augments the lethality (MIC) of mycobacterial agents [17-20].

The lack of the human homolog of this protein coupled with sequence variations at the mycobacterial menaquinol binding site, in comparison to bacterial homologs, presents an opportunity to target these residues selectively in mycobacteria. This would also allow target selectivity as well as to push the mycobacteria into a suicidal mode, when used in combination therapy and avoid mycobacterial drug resistance. In this study, we present the identification of a novel mycobacterial *cyt-bd* inhibitor, MQ-H₂ that targets the mycobacterial menaquinol loop region and inhibits ATP synthesis in *M. smegmatis* inverted membrane vesicles (IMVs). Further, by employing differential substrates (NADH₂ or succinate) and IMVs of the cytochrome *bcc* deficient *M. smegmatis* mutant (Δbcc) we showed, that MQ-H₂ inhibits mycobacterial ATP synthesis proposed by targeting the terminal *cyt-bd*.

Materials & Methods

Modeling simulations

Homology modeling: To our knowledge, neither high- nor low resolution structures of mycobacterial *cyt-bd* have been determined. We have utilized comparative protein or homology modeling as a work around to obtain the 3D structural model of the *M. tuberculosis* (*Mtb*) *cyt-bd*. Using protein blast, the closest homolog of *Mtb* *cyt-bd* were enumerated and the closest homolog *G. thermodenitrificans* *cyt-bd* (pdb 5DOQ, resolved at 3.05 Å) with 27.0 percent identity [16] was employed as a template to model *Mtb* *cyt-bd* structures using Phyre² (Protein Homology/analogY Recognition Engine V 2.0) [18].

Protein Preparation: The *Mtb* homology model of *cyt-bd* was prepared by fixing the bond orders of the cofactors - porphyrin rings, heme atoms and the ligated histidine residue during the refine step of protein preparation. The refined protein was energy minimized until the heavy atoms converged to 0.3 Å rmsd using OPLS force field in protein preparation wizard and Macromodel modules in Schrödinger suite of programs [22, 23]. The quality of the homology model was evaluated using procheck algorithm [24, 25]. All molecular modeling simulations were performed on a Linux workstation.

Ligand preparation: Chemdiv discovery collection of more than one million molecules was employed for virtual screening studies. Using default settings with ligand preparation and energy minimization tools, the 2D library was converted into 3D and energy minimized. The mycobacterial specific residues such as M251, M259, F274, S275, S340, and M348 that make up the substrate binding were used to define the site point for grid generation using default settings in glide. The Chemdiv 3D library was run through High-Throughput Virtual Screening (HTVS) mode, the Standard Precision (SP) mode, and extra precision (XP) mode using default settings [26, 27]. The best scoring poses were selected based on their interactions at the above predefined residues as well as heme *b558*. Qikprop tool [15] was used to calculate the absorption, distribution, metabolism, excretion and toxicity (ADMET) properties and together with properties and Glide scores, 10 best probable ligands are selected for purchase.

ATP synthesis assays

Preparation of the wild type (WT) *M. smegmatis* mc² 155- and Δbcc *M. smegmatis* IMVs was done as described previously [28] and ATP synthesis was performed according to Hotra et al., 2016 [29] in 96 well plates. ATP synthesis (%) in the presence of varying concentrations of compound was compared to untreated wells as negative control. Dose response inhibition (IC₅₀) values were determined by using variable slope (four parameters) non-linear regression fitting model (IC₅₀ ± S.D) in GraphPad software 8.0 [30]. The *M. smegmatis* Δbcc mutant, deficient of the gene encoding the mycobacterial cytochrome *bcc* complex was kindly provided by Professor Gregory M. Cook, Department of Microbiology and Immunology, School of Biomedical Sciences, University of Otago, Dunedin 9054, New Zealand.

Results & Discussion

Homology model of Cyt bd Oxidase

Blast protein search for homologues of cyt-*bd* oxidase on the protein database revealed the *G. thermodenitrificans* cyt-*bd* oxidase structure with a resolution of 3.05 Å as the closest homolog with a sequence identity of 27%. The sequence alignment with this template showed borderline positives of 45% and a low percentage of gaps (10%) suggesting that a reasonable homology model could be built (data not shown). We utilized the *ab initio* algorithm in Phyre² program, which can efficiently generate a homology model for sequences with low sequence identity, and generated an ensemble of models. The quality of the homology models was evaluated by procheck algorithm [24, 25]. The Ramachandran plot suggested that ~91 percent of the residues were in the most favorable region, 18 and 0.5% of the residues in additional and generously allowed regions respectively and 0% residues in disallowed regions (Supplementary Fig. S2). The model had an overall G-factor of -0.17 which was above the specified cutoff of -0.5, suggesting that the model built was of reasonable stereochemical quality.

Mycobacterial cyt-bd specific epitopes within the redox center and the menaquinol-binding site

An amino acid sequence comparison of bacterial and mycobacterial cyt-*bd* oxidases highlights that the bacterial cyt-*bd* employs a histidine and methionine residues as bi-axial ligands for heme *b*558 coordination. In *E. coli*, glutamate residues such as E99, E107 (anchoring heme *b*595) (Supplementary Fig. S2) were shown to mediate oxygen channel formation and are a prerequisite for terminal oxidation of oxygen to water. Further, mutagenesis data on the menaquinol loop region (E257A, (heme *b*558)) of the *E. coli* cyt-*bd* oxidase highlighted the possibility of differential regulation of oxidase activity without the loss of *b*595 and *d* hemes [11]. Strikingly, the menaquinol loop binding region in mycobacterial species has multiple residues that are varied in comparison to bacterial orthologues. Mainly, the residues such as H185, D245, M251, F252, M257, M259, F274, S275, V297, S340, M343, M344, M348, and V393 (Fig. 1, light pink shaded) that outline the menaquinol binding site are unique compared to bacterial orthologues. Another conspicuous feature is the presence of methionine residues around the catalytic site in mycobacterial cytochrome oxidase enzyme. This highlights the possibility of surface exposed methionine residues guarding the enzyme from excess of ROS by serving as scavengers of ROS [31, 32]. These peculiar features inside the mycobacterial menaquinol binding site present the avenue to enrich selectivity towards the mycobacterial cyt-*bd* oxidase.

Identification of novel ligands

These intriguing features at the menaquinol binding loop region motivated us to carry out a virtual screening campaign to identify novel chemical entities that could bind the highlighted residues and inhibit mycobacterial *cyt-bd* oxidase and with this oxidative phosphorylation. As depicted in Figure 2, our initial glide high throughput virtual screening (HTVS) enabled us to differentiate between probable binders and non-binders from a library of more than one million molecules. The ligands with a docking score of less than -5.0 only were taken forward into a standard precision run. This run carried out an exhaustive conformation sampling of ligand torsions to generate pose conformations. Poses with docking score of less than -6.0 were taken further into extra precision run. Glide XP uses much more exhaustive approach of "anchor and grow" to sample the conformational space and a XP scoring function to yield the best ranking poses. Next, ADMET properties were enumerated using Qikprop tool to further exclude ligands with unfavorable solubility, logP, and Human Ether-a-go-go-Related Gene (HERG) binding predictions. Finally, pose interaction analysis enabled us to identify ten ligands that are predicted to bind with sub-micromolar affinity at the previously highlighted *Mtb* *cyt-bd* residues.

Potency and target specificity of the novel compound MQL-H₂

We evaluated the ability of compounds to inhibit mycobacterial ATP synthesis using IMVs of WT *M. smegmatis* and the Δbcc mutant strain at 1 and 100 μ M concentrations (data not shown). Among these 10 compounds, compound (MQL-H₂), 3-[[2-(4-chlorophenyl)ethylamino]methyl]-1-ethyl-indole-2-carboxylic acid inhibited NADH-driven ATP synthesis of IMVs of WT *M. smegmatis* with an IC₅₀ of $60 \pm 4.3 \mu$ M (*red line*, Fig. 3a) while the positive control Q203 showed an IC₅₀ of 1.6 ± 0.3 nM (*blue line*, Fig. 3a). Likewise, MQL-H₂ also exhibited the ability to inhibit succinate-driven ATP synthesis with an IC₅₀ $75 \pm 2.5 \mu$ M in comparison to the control of Q203 (IC₅₀ 0.9 ± 0.4 nM) (Fig. 3b, *blue line*). Since varying the electron donors that activate ATP synthesis via complex I and -II have not abrogated the inhibitory effects of MQL-H₂, it can be inferred that both complexes were not involved in mediating the actions of MQL-H₂. Furthermore, our results with Δbcc *M. smegmatis* IMVs also showed that MQL-H₂ inhibited ATP synthesis with an IC₅₀ $34 \pm 1.7 \mu$ M (Fig. 3c). Taken together, the ability of MQL-H₂ to inhibit the ATP synthesis in Δbcc *M. smegmatis* IMVs corroborates that cytochrome *bcc* reductase was not involved in mediating the actions of MQL-H₂ and more likely points to the role of terminal *cyt-bd* oxidase as probable target as envisaged in our drug design.

Molecular interactions of MQL-H₂ with the menaquinol loop of mycobacterial cyt-bd

The structure of MQL-H₂ has two aromatic rings linked by an ethyl-amino-methyl fragment to the 3rd position of N-ethyl-indole-2-carboxylic acid (Fig. 3d). Our molecular docking results revealed that the indole fragment docked deeply into the substrate binding site with a glide gscore of -6.6, suggestive of being a micro-molar binder (Fig. 4). The phenyl moiety of indole is docked into the vicinity of the heme *b*558 group and was engaged in strong hydrophobic interactions (*pink line*) with the amino acids M259, F252 and G248. The N1-ethyl on indole ring seems to anchor hydrophobic interactions with the side chain atoms of M344 of the enzyme. Further, the indole aromatic ring was involved in i) strong π - π stacking interactions (*orange line*) with F274, ii) π -alkyl interactions (*pink line*) with the heme *b*558 group, and iii) π -sulfur interactions (*pink line*) with residue M344. The amino linker interacts with the acid moiety of D245 via attractive electrostatic charged interaction, while the ethyl hydrogen atoms have van der Waals contacts with the D245 acid moiety (not shown for clarity). The terminal chlorophenyl group on this ligand was also engaged in π -alkyl interactions with the heme *b*558 group (*pink lines*) while the 4-chloro atom on the phenyl has hydrophobic interactions (*pink line*, (~3 Å)) with β -methylene (CH₂) atoms of M348.

Conclusions

Mycobacteria have evolved to survive regulate respiration by enhancing alternate oxidases such as *cyt-bd* and survive even in extreme conditions. In this study, we employed an *in silico* screening to identify a novel inhibitor MQL-H₂ that targets mycobacterial *cyt-bd* at the menaquinol-binding site. MQL-H₂ inhibited the ATP synthesis driven by differential electron donor substrates as well as in *Abcc M. smegmatis* IMVs. Together with molecular docking, the biochemical assays revealed that the efficacy of MQL-H₂ in oxidative phosphorylation inhibition is mediated via selective inhibition of the terminal *cyt-bd*. These novel findings pave the way for medicinal chemistry based hit optimization efforts of MQL-H₂.

Acknowledgements:

This research was supported by the National Research Foundation (NRF) Singapore, NRF Competitive Research Programme (CRP), Grant Award Number NRF-CRP18-2017-01). S. S. M. C. is grateful for an NTU research scholarship at Nanyang Technological University.

Conflict of interest

The authors declare no conflict of interest.

References

1. WHO World Health Organization Global tuberculosis report 2019. https://www.who.int/tb/publications/global_report/en/. doi: https://www.who.int/tb/publications/global_report/GraphicExecutiveSummary.pdf?ua=1
2. Working Group (2019) FDA approves new drug for treatment-resistant forms of tuberculosis in, Working Group on New Drugs, New York, USA.
3. Tang S, Yao L, Hao X, Liu Y, Zeng L, Liu G, Li M, Li F, Wu M, Zhu Y, Sun H, Gu J, Wang X and Zhang Z (2015) Clofazimine for the treatment of multidrug-resistant tuberculosis: prospective, multicenter, randomized controlled study in China. *Clin Infect Dis* 60:1361-7. doi: 10.1093/cid/civ027
4. Pethe K, Bifani P, Jang J, Kang S, Park S, Ahn S, Jiricek J, Jung J, Jeon HK, Cechetto J, Christophe T, Lee H, Kempf M, Jackson M, Lenaerts AJ, Pham H, Jones V, Seo MJ, Kim YM, Seo M, Seo JJ, Park D, Ko Y, Choi I, Kim R, Kim SY, Lim S, Yim SA, Nam J, Kang H, Kwon H, Oh CT, Cho Y, Jang Y, Kim J, Chua A, Tan BH, Nanjundappa MB, Rao SP, Barnes WS, Wintjens R, Walker JR, Alonso S, Lee S, Kim J, Oh S, Oh T, Nehrbass U, Han SJ, No Z, Lee J, Brodin P, Cho SN, Nam K and Kim J (2013) Discovery of Q203, a potent clinical candidate for the treatment of tuberculosis. *Nat Med* 19:1157-60. doi: 10.1038/nm.3262
5. FDA (2012) SIRTUO™ (bedaquiline). doi: https://www.accessdata.fda.gov/drugsatfda_docs/label/2013/204384s002lbl.pdf
6. Sutherland HS, Tong AST., Choi PJ, Conole D, Blaser A, Franzblau SG., Cooper CB, Upton A M, Lotlikar MU, Denny WA and Palmer BD (2018) Structure-activity relationships for analogs of the tuberculosis drug bedaquiline with the naphthalene unit replaced by bicyclic heterocycles. *Bioorg Med Chem.* 26, 1797-1809. doi: 10.1016/j.bmc.2018.02.026
7. Blaser A, Sutherland HS, Tong AST, Choi PJ, Conole D, Franzblau SG, Cooper CB, Upton A M, Lotlikar M, Denny WA and Palmer BD (2019) Structure-activity relationships for unit C pyridyl analogues of the tuberculosis drug bedaquiline. *Bioorg Med Chem.* 27, 1283-1291. doi: 10.1016/j.bmc.2019.02.025
8. Bald D, Villellas C, Lu P and Koul A (2017) Targeting Energy Metabolism in Mycobacterium tuberculosis, a New Paradigm in Antimycobacterial Drug Discovery. *MBio* 8. doi: 10.1128/mBio.00272-17
9. Safarian S, Hahn A, Mills DJ, Radloff M, Eisinger ML, Nikolaev A, Meier-Credo J, Melin F, Miyoshi H, Gennis RB, Sakamoto J, Langer JD, Hellwig P, Kühlbrandt W and Michel H (2019) Active site rearrangement and structural divergence in prokaryotic respiratory oxidases. *Science* 366:100. doi: 10.1126/science.aay0967
10. Belevich I, Borisov VB, Zhang J, Yang K, Konstantinov AA, Gennis RB and Verkhovsky MI (2005) Time-resolved electrometric and optical studies on cytochrome *bd* suggest a mechanism of electron-proton coupling in the di-heme active site. *Proceedings of the National Academy of Sciences of the United States of America* 102:3657-3662. doi: 10.1073/pnas.0405683102
11. Yang K, Zhang J, Vakkasoglu AS, Hielscher R, Osborne JP, Hemp J, Miyoshi H, Hellwig P and Gennis RB (2007) Glutamate 107 in subunit I of the cytochrome *bd* quinol oxidase from *Escherichia coli* is protonated and near the heme d/heme b595 binuclear center. *Biochemistry* 46:3270-8. doi: 10.1021/bi061946+
12. Safarian S, Rajendran C, Muller H, Preu J, Langer JD, Ovchinnikov S, Hirose T, Kusumoto T, Sakamoto J and Michel H (2016) Structure of a *bd* oxidase indicates similar mechanisms for membrane-integrated oxygen reductases. *Science* 352:583-6. doi: 10.1126/science.aaf2477

13. Aung HL, Berney M and Cook GM (2014) Hypoxia-activated cytochrome bd expression in *Mycobacterium smegmatis* is cyclic AMP receptor protein dependent. *J Bacteriol* 196:3091-7. doi: 10.1128/JB.01771-14
14. Megehee JA, Hosler JP and Lundrigan MD (2006) Evidence for a cytochrome bcc-aa3 interaction in the respiratory chain of *Mycobacterium smegmatis*. *Microbiology* 152:823-829. doi: <https://doi.org/10.1099/mic.0.28723-0>
15. Forte E, Borisov VB, Davletshin A, Mastronicola D, Sarti P and Giuffre A (2013) Cytochrome bd oxidase and hydrogen peroxide resistance in *Mycobacterium tuberculosis*. *MBio* 4:e01006-13. doi: 10.1128/mBio.01006-13
16. Giuffre A, Borisov VB, Mastronicola D, Sarti P and Forte E (2012) Cytochrome bd oxidase and nitric oxide: from reaction mechanisms to bacterial physiology. *FEBS Lett* 586:622-9. doi: 10.1016/j.febslet.2011.07.035
17. Berney M, Hartman TE and Jacobs WR, Jr. (2014) A *Mycobacterium tuberculosis* cytochrome bd oxidase mutant is hypersensitive to bedaquiline. *MBio* 5:e01275-14. doi: 10.1128/mBio.01275-14
18. Kalia NP, Hasenoehrl EJ, Ab Rahman NB, Koh VH, Ang MLT, Sajorda DR, Hards K, Grüber G, Alonso S, Cook GM, Berney M and Pethe K (2017) Exploiting the synthetic lethality between terminal respiratory oxidases to kill *Mycobacterium tuberculosis* and clear host infection. *Proc Natl Acad Sci U S A* 114:7426-7431. doi: 10.1073/pnas.1706139114
19. Moosa A, Lamprecht DA, Arora K, Barry CE, 3rd, Boshoff HIM, Ioerger TR, Steyn AJC, Mizrahi V and Warner DF (2017) Susceptibility of *Mycobacterium tuberculosis* Cytochrome bd Oxidase Mutants to Compounds Targeting the Terminal Respiratory Oxidase, Cytochrome c. *Antimicrob Agents Chemother* 61. doi: 10.1128/AAC.01338-17
20. Mascolo L and Bald D (2019) Cytochrome bd in *Mycobacterium tuberculosis*: A respiratory chain protein involved in the defense against antibacterials. *Prog Biophys Mol Biol*. doi: 10.1016/j.pbiomolbio.2019.11.002
21. Lu P, Asseri AH, Kremer M, Maaskant J, Ummels R, Lill H and Bald D (2018) The anti-mycobacterial activity of the cytochrome bcc inhibitor Q203 can be enhanced by small-molecule inhibition of cytochrome bd. *Sci Rep* 8:2625. doi: 10.1038/s41598-018-20989-8
22. Madhavi Sastry G, Adzhigirey M, Day T, Annabhimoju R and Sherman W (2013) Protein and ligand preparation: parameters, protocols, and influence on virtual screening enrichments. *Journal of Computer-Aided Molecular Design* 27:221-234. doi: 10.1007/s10822-013-9644-8
23. Schrödinger Release 2019-2: Maestro, Force Fields, MacroModel, Prime, Protein Preparation Wizard, Ligprep, ConfGen, Phase, QikProp, Glide. Schrödinger, LLC, New York, NY, 2019.
24. Laskowski RA, Rullmannn JA, MacArthur MW, Kaptein R and Thornton JM (1996) AQUA and PROCHECK-NMR: programs for checking the quality of protein structures solved by NMR. *J Biomol NMR* 8:477-86. doi: 10.1007/bf00228148
25. Ramachandran GN, Ramakrishnan C and Sasisekharan V (1963) Stereochemistry of polypeptide chain configurations. *J Mol Biol* 7:95-9. doi: 10.1016/s0022-2836(63)80023-6
26. Friesner RA, Banks JL, Murphy RB, Halgren TA, Klicic JJ, Mainz DT, Repasky MP, Knoll EH, Shelley M, Perry JK, Shaw DE, Francis P and Shenkin PS (2004) Glide: a new approach for rapid, accurate docking and scoring. 1. Method and assessment of docking accuracy. *J Med Chem* 47:1739-49. doi: 10.1021/jm0306430
27. Friesner RA, Murphy RB, Repasky MP, Frye LL, Greenwood JR, Halgren TA, Sanschagrin PC and Mainz DT (2006) Extra precision glide: docking and scoring incorporating a model of hydrophobic enclosure for protein-ligand complexes. *J Med Chem* 49:6177-96. doi: 10.1021/jm051256o
28. Lu P, Heineke MH, Koul A, Andries K, Cook GM, Lill H, van Spanning R and Bald D (2015) The cytochrome bd-type quinol oxidase is important for survival of *Mycobacterium smegmatis* under peroxide and antibiotic-induced stress. *Sci Rep* 5:10333. doi: 10.1038/srep10333
29. Hotra A, Suter M, Biukovic G, Ragunathan P, Kundu S, Dick T and Grüber G (2016) Deletion of a unique loop in the mycobacterial F-ATP synthase gamma subunit sheds light on its inhibitory role in ATP hydrolysis-driven H(+) pumping. *FEBS J* 283:1947-61. doi: 10.1111/febs.13715

30. (2019) Dose response inhibition using four parameter variable slope non-linear regression was performed using GraphPad Prism version 8.00 for Windows, GraphPad Software, La Jolla California USA, “www.graphpad.com”.
31. Levine RL, Mosoni L, Berlett BS and Stadtman ER (1996) Methionine residues as endogenous antioxidants in proteins. *Proc Natl Acad Sci U S A* 93:15036-40. doi: 10.1073/pnas.93.26.15036
32. Kim G, Weiss SJ and Levine RL (2014) Methionine oxidation and reduction in proteins. *Biochim Biophys Acta* 1840:901-5. doi: 10.1016/j.bbagen.2013.04.038

Fig. 1 Sequence alignment of the mycobacterial *cyt-bd* menaquinol loop region with other homologue enzymes.

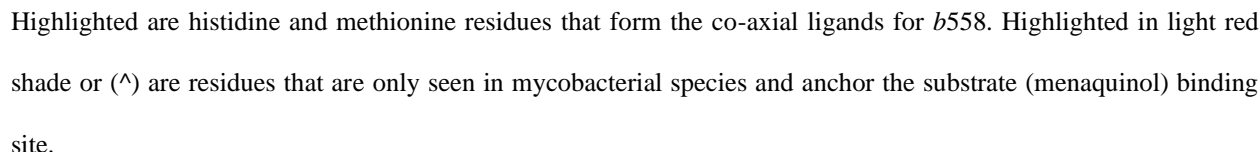


Figure 2

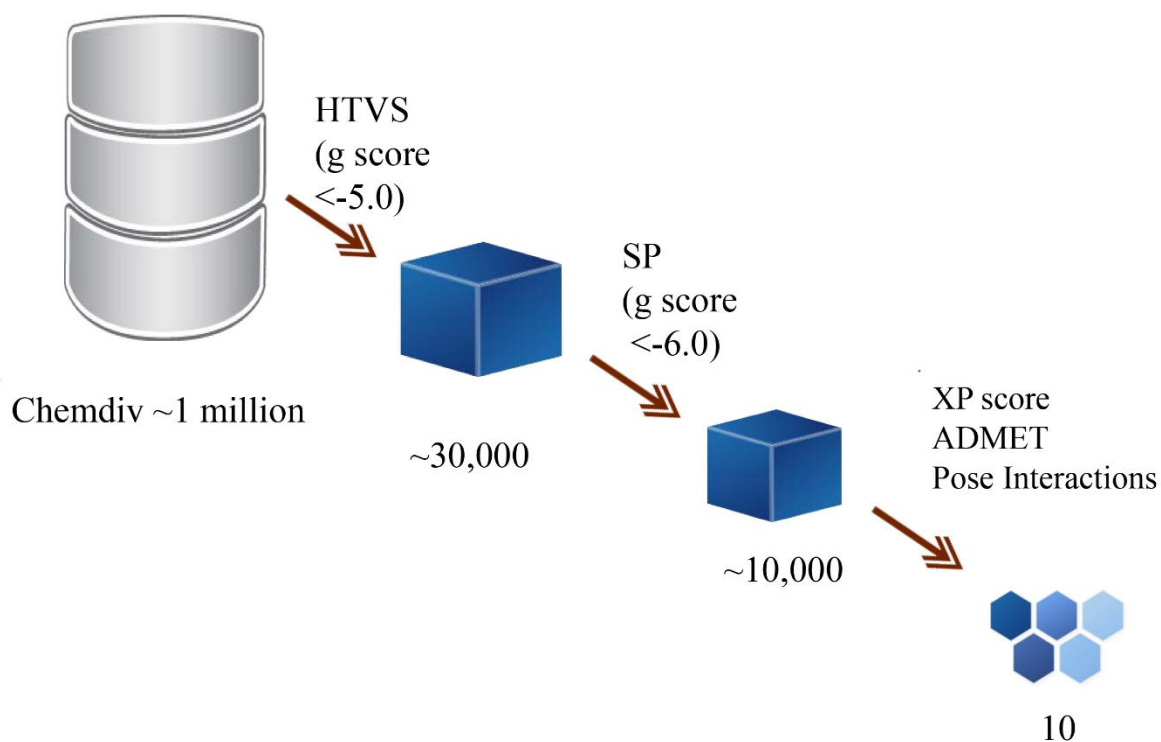


Fig. 2 Flow chart showing the steps used in virtual screening. High throughput virtual screening (HTVS) using of Chemdiv's ~1 million discovery collection led to differentiate the binders. Molecules with a g-score of < -5.0 were taken into standard precision (SP) run. Next, using a cutoff g-score of < -6 were considered for extra precision (XP) run. Using XP score, pose interactions at the intended residues and ADMET property filters led to finalizing 10 ligands for purchase.

Figure 3

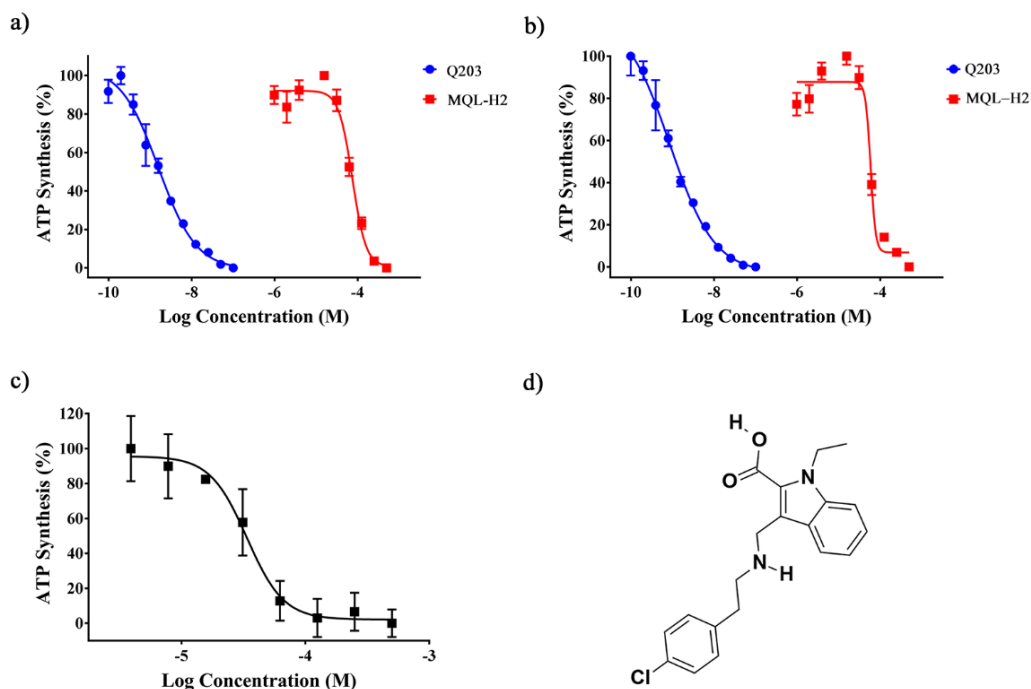


Fig. 3 Effects of MQL-H2 on ATP synthesis. a) Dose response curve of MQL-H₂ ($IC_{50} 60 \pm 4.3 \mu M$) showing the inhibition of NADH₂ driven ATP synthesis on WT *M. smegmatis* IMVs compared to Q203 ($IC_{50} 1.6 \pm 0.3 nM$). b) Dose response curve of MQL-H₂ ($IC_{50} 75 \pm 2.5 \mu M$) revealing the inhibition of succinate-driven ATP synthesis on WT *M. smegmatis* IMVs compared to Q203 ($IC_{50} 0.9 \pm 0.4 nM$). c) Dose response curve of MQL-H₂ ($IC_{50} 34 \pm 1.7 \mu M$) demonstrating the inhibition of NADH-driven ATP synthesis on the *M. smegmatis* Δbcc mutant IMVs. d) Chemical structure of MQL-H₂ bears the IUPAC name of 3-[[2-(4-chlorophenyl)ethylamino]methyl]-1-ethyl-indole-2-carboxylic acid.

Figure 4

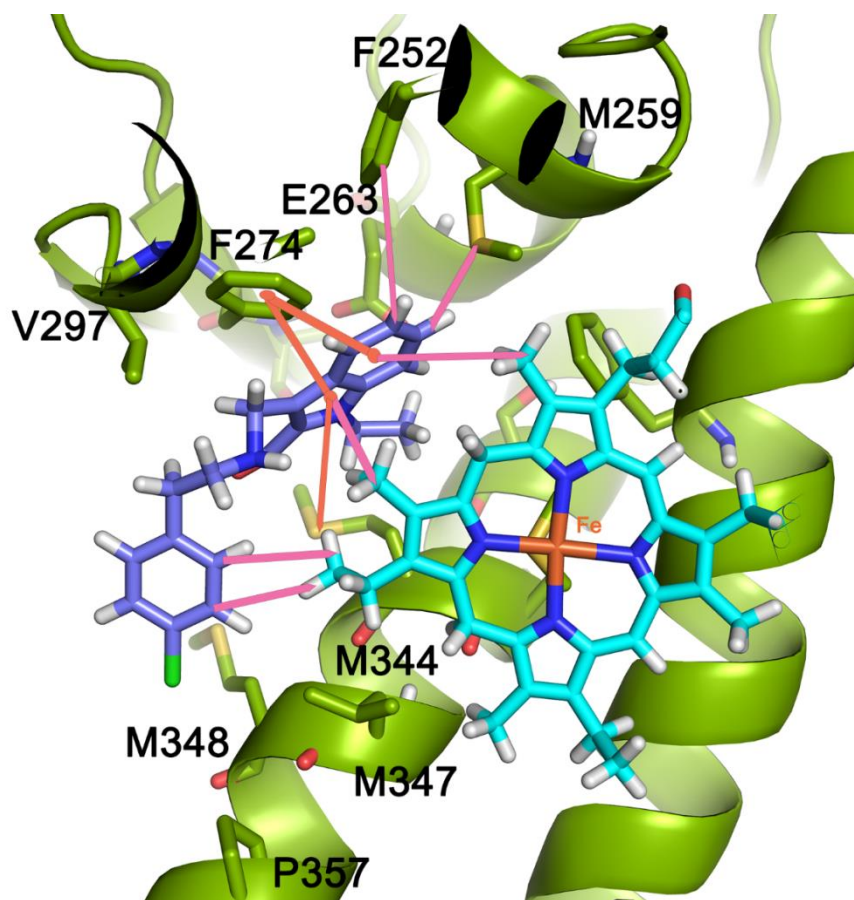


Fig. 4 Cartoon model of MQL-H₂-binding at the MQ-loop region of *Mtb* cyt-*bd*. The indole ring on MQL-H₂ has π - π stacking interaction (orange line) with F274 and π -alkyl interaction with heme *b*558 (pink line), M344 (π -S, orange line) highlight that this ligand is deeply positioned into the quinol binding site. Shown in pink are alkyl hydrophobic interactions of the indole ring with M259, F253 interactions. The N₁ ethyl on indole ring also further chaperone the alkyl interactions with side chain atoms of M344. The terminal chlorophenyl ring was also involved in alkyl interaction with the heme *b*558 group and M348 residues (pink line). The linker amino atom mediates the electrostatic charged interaction with acid moiety of D245 (*not shown for clarity*). Proximal histidine is also not shown for clarity.